

Modelling gas heating in air plasmas

C. D. Pintassilgo^{1,2} and V. Guerra¹

¹*Instituto de Plasmas e Fusão Nuclear, Instituto Superior Técnico,
Universidade de Lisboa, Lisboa, Portugal*

²*Departamento de Engenharia Física, Faculdade de Engenharia,
Universidade do Porto, Porto, Portugal*

This work presents simulations of the gas temperature in air plasma discharges for different values of the reduced electric field, electron density, pressure and tube radius. The study is based on the solutions to the time-dependent gas thermal balance coupled to the vibrational and chemical kinetic equations for the most important heavy-species produced in these plasmas. Modelling results show that gas heating is faster when the reduced electric field and electron density increase as a result of more efficient electronic collisions, $e + O_2 \rightarrow e + 2O(^3P)$ and $\dots \rightarrow e + O(^3P) + O(^1D)$, recombination of oxygen atoms at the wall and V-T N_2 -O collisions. This last process is also responsible for an increase of the gas temperature with the pressure and tube radius.

1. Introduction

The purpose of this work is to provide a detailed time-dependent study of gas heating mechanisms in air (N_2 -20% O_2) plasma discharges in cylindrical geometry for different values of reduced electric field E/N_g (where N_g is the gas number density) and electron density n_e , as well as several working plasma conditions, such as pressure and tube radius.

Our simulations involve a time range from 0.01 to 100 ms, E/N_g values varying from 50 up to 300 Td and electron densities between 10^9 and 10^{11} cm⁻³. In parallel, we analyse the role of pressure p and tube radius R by considering respectively $p = 1, 10, 20$ Torr and $R = 0.5, 1, 1.5$ cm.

2. Model

2.1. Gas temperature

It is assumed isobaric conditions on a discharge tube where the plasma is axially homogeneous and the heat conduction is the dominant cooling mechanism. Moreover, considering a parabolic profile with temperatures T_0 and T_w , respectively, at the tube axis and at the wall, the time-dependent equation for the the radially averaged gas temperature T_g , may be given by [1]

$$n_m c_p \frac{\partial T_g}{\partial t} = \frac{8\lambda_g(T_w - T_g)}{R^2} + Q_{in}, \quad (1)$$

where n_m and c_p are, respectively, the molar density and the molar heat capacity at constant pressure. Under these conditions, the temperature at the axis T_0 is given by $2T_g - T_w$. While the first term on the right hand side of this equation represents the gas cooling mechanism for a spatially homogeneous

thermal conductivity λ_g in a tube with radius R , the second term Q_{in} corresponds to the average total net power transferred per unit volume into gas heating from the energy release in volume and wall processes [2].

In air plasmas, these processes may result from electronic collisions with N_2 and O_2 via the following gas heating mechanisms:

- (1) Elastic collisions of electrons with N_2 and O_2 molecules;
- (2) Nitrogen and oxygen dissociation by electron impact collisions through pre-dissociative states N_2^* and O_2^* ;
- (3) Electron-ion recombination involving nitrogen or oxygen ions,

together with the contribution of vibrational and chemical kinetics to gas heating, since our simulations deal with time ranges longer than 1 ms, through the following processes:

- (4) Non-resonant V-V energy exchanges in $N_2 - N_2$ and $N_2 - O_2$ collisions;
- (5) V-T energy exchanges in $N_2 - N_2$, $N_2 - O_2$, $N_2 - O$ and $N_2 - N$ collisions;
- (6) Vibrational deactivation of $N_2(X, v)$ at the wall;
- (7) Exothermic chemical reactions;
- (8) Diffusion of molecular and atomic metastables states to the wall;
- (9) Recombination of N and O atoms at the wall.

The expressions for the heating rates and available energy for gas heating concerning these processes have been presented and discussed in [1].

2.2. Kinetic model

Our kinetic model is based on the solutions of equation (1) coupled to a system of time-dependent rate balance equations describing the kinetics of the most important heavy species produced in low-pressure N_2 -20% O_2 plasmas. We consider 45 vibrationally excited states of ground state molecular nitrogen $N_2(X^1\Sigma_g^+, v)$, the electronically excited states $N_2(A^3\Sigma_u^+, B^3\Pi_g, B^3\Sigma_u^-, C^3\Pi_u, a^1\Sigma_u^-, a^1\Pi_g, w^1\Delta_u)$ and $O_2(a^1\Delta_g, b^1\Sigma_g^+)$, both ground and excited states of atomic nitrogen $N(^4S, ^2D, ^2P)$, atomic oxygen on the ground state $O(^3P)$ and excited state $O(^1D)$, other chemical neutral species produced by chemical reactions, such as $NO(X^2\Pi, A^2\Sigma^+, B^2\Pi)$, $NO_2(X, A)$ and O_3 , the main positive ions $N_2^+, N_4^+, O_2^+, O^+, NO^+$ and the negative ion O^- .

In order to ensure the coupling between electron, vibrational and chemical kinetics, we consider the set of electron coefficients and parameters obtained from the electron Boltzmann equation for a certain value E/N_g and N_2 vibrational distribution function (VDF) that leads to the same VDF after solving the system of rate balance equations for a given value of the electron density n_e .

3. Results and discussion

Figures 1 and 2 report the results of our simulations for the time-evolution of the radially averaged gas temperature T_g in air plasmas with a pressure of 1 Torr in a tube radius of 1 cm for different values of E/N_g and n_e .

These two figures reveal a faster gas heating and larger values of T_g when E/N_g and n_e increase. This effect is, on one hand, a consequence of more efficient electronic impact collisions, which lead to an increase of the gas heating rate of electronic impact processes $e + O_2 \rightarrow e + 2O(^3P)$ and $e + O_2 \rightarrow e + O(^3P) + O(^1D)$ and, on the other hand, as the populations of oxygen atoms become larger, there is also an increase of the contribution to gas heating from V-T N_2 -O collision processes, recombination of O atoms at the wall and in a lesser extent, process $N_2(A) + O \rightarrow NO(X) + N(^2D)$.

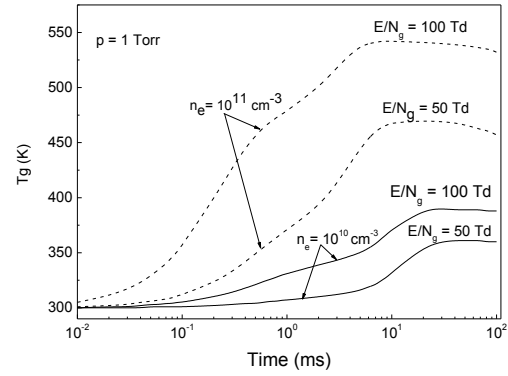


Figure 1. Temporal variation of the radially averaged gas temperature T_g in a N_2 -20% O_2 discharge with $p = 1$ Torr in a tube radius of 1 cm for a reduced electric field E/N_g of 50 and 100 Td, when the electron density n_e is 10^{10} cm^{-3} (full curves) and 10^{11} cm^{-3} (dashed curves).

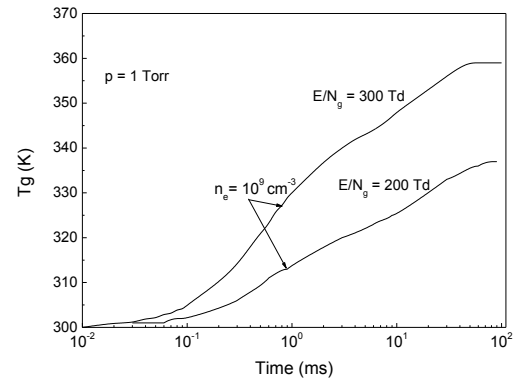


Figure 2. Temporal variation of the radially averaged gas temperature T_g in a N_2 -20% O_2 discharge with $p = 1$ Torr in a tube radius of 1 cm for a reduced electric field E/N_g of 200 and 300 Td, when the electron density n_e is 10^9 cm^{-3} .

Figure 3 plots the temporal variation of T_g for $E/N_g = 300$ Td and $n_e = 10^9$ cm^{-3} in an air plasma produced in a tube with $R = 1$ cm for three different pressures: 1, 10 and 20 Torr. One may observe from this figure that the gas temperature increases as the pressure becomes larger, under the conditions assumed in this work. A detailed analysis of the contribution of the most important gas heating mechanisms (not shown here) shows that this behaviour is essentially a consequence of more important V-T N_2 -O collisions, since both $[N_2(X, v)]$ and $[O(^3P)]$ increase with pressure.

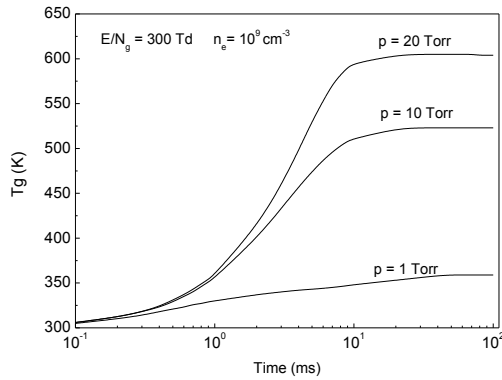


Figure 3. Temporal variation of the radially averaged gas temperature T_g in a N_2 -20% O_2 discharge with a tube radius of 1 cm, when $E/N_g = 300$ Td and $n_e = 10^9$ cm^{-3} for the following values of pressure: $p = 1, 10$ and 20 Torr.

The role of the tube radius R on gas heating is reported in figure 4, where we plot the time-dependent evolution of the gas temperature for an air plasma discharge when $E/N_g = 100$ Td and $n_e = 10^{10}$ cm^{-3} for $R = 0.5, 1$ and 1.5 cm.

This figure shows a faster gas heating as R increases. For the larger values of this parameter, the population of oxygen atoms increases due to a smaller role played by their recombination at the wall. At the same time, there is a decrease in the importance of the cooling mechanism represented in the first term on the right-hand side of equation (1). Hence, the behaviour plotted in figure 4 is mainly a result of the combined effect of more efficient V-T N_2 -O collisions with a smaller magnitude of the cooling mechanism.

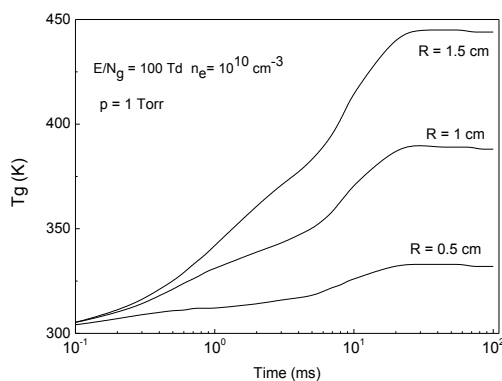


Figure 4. Temporal variation of the radially averaged gas temperature T_g in a N_2 -20% O_2 pulsed at a pressure of 1 Torr when $E/N_g = 100$ Td and $n_e = 10^{10}$ cm^{-3} for the following values of the tube radius: $R = 0.5, 1$ and 1.5 cm.

3. Concluding remarks

We have presented modelling results for the temporal evolution of the gas temperature in air-like (N_2 -20% O_2) plasmas discharges for different values of reduced electric field, electron density, pressure and tube radius. Our simulations give a detailed description on the time-dependent variation of the gas temperature for different plasma conditions, providing also an insight of the most important gas heating channels.

4. Acknowledgements

Work partially supported by the Portuguese FCT-Fundação para a Ciência e a Tecnologia, under Project UID/FIS/50010/2013.

5. References

- [1] C.D. Pintassilgo, V. Guerra, O. Guaitella, A. Rousseau *Plasma Sources Sci. Technol.* **23** (2014) 025006
- [2] N.A. Popov, *J. Phys. D. Appl. Phys.* **44** (2011) 285201